1   **Contribution of the Sensitivity Analysis in Groundwater Vulnerability Assessing Using the**

2   **DRASTIC and Composite DRASTIC Indexes**

3   Mohammad Malakootian[1], Majid Nozari[2],*

4   **Manuscript Authors details:**

5   1. Mohammad Malakootian, Department of Environmental Health, School of Public Health,

6   Kerman University of Medical Sciences, Iran. E-mail: m.malakootian@yahoo.com.

7   https://orcid.org/0000-0002-4051-6242.

8   2. Majid Nozari, Department of Environmental Health, School of Public Health, Kerman

9   University of Medical Sciences, Iran. Tel: 98-9383921819, E-mail: nozari.m@kmu.ac.ir.

10   https://orcid.org/0000-0003-2319-1930.

23 **ABSTRACT**

24 The present study estimates Kerman–Baghin aquifer vulnerability by applying the DRASTIC

25 and composite DRASTIC (CDRASTIC) indexes. The factors affecting the transfer of

26 contamination, including the water table depth, soil media, aquifer media, the impact of the

27 vadose zone, topography, hydraulic conductivity, and land use, were ranked, weighted, and

28 integrated using a geographical information system (GIS). A sensitivity test has also been

29 performed to specify the sensitivity of the parameters. The study results show that the

30 topographic layer displays a gentle slope in the aquifer. The majority of the aquifer covered

31 irrigated field crops and grassland with a moderate vegetation cover. In addition, the aquifer

32 vulnerability maps indicate very similar results, recognizing the northwest parts of the aquifer as

33 areas with high and very high vulnerability. The map removal sensibility analysis (MRSA)

34 revealed the impact of the vadose zone (in the DRASTIC index) and hydraulic conductivity (in

35 the CDRASTIC index) as the most effective parameters in the vulnerability evaluation. In both

36 indexes, the single-parameter sensibility analysis (SPSA) showed net recharge as the most

37 effective factor in the vulnerability estimation. From this study, it can be concluded that

38 vulnerability maps can be used as a tool to control human activities for the sustained protection

39 of aquifers.

40

41 **Keywords:** Vulnerability; Sensitivity analyses; DRASTIC; Composite DRASTIC; Kerman–

42 Baghin aquifer

43

44

45

46

1. Introduction

47

48   Groundwater̶'̶s̶ ̶a̶r̶e̶ as a significant and principal resource in most parts of the world, especially

49   for those in waterless and arid areas. Water quality has been given more affirm on groundwater's

50   control (Neshat et al., 2014;Manap et al., 2013;Manap et al., 2014a;Ayazi et al., 2010). The

51   potential groundwater's contamination by mankind operations at or near the surface of the

52   groundwater has been supposed the major base for control of this source (Tilahun and Merkel,

53   2010).

54   The introduction of potential contaminants to a location on top of an aquifer at a s̶p̶e̶c̶i̶f̶i̶e̶d̶

55   p̶o̶s̶i̶t̶i̶o̶n̶ in an underground system is defined as groundwater vulnerability (Sarah and Patricia l,

56   1993;Neshat et al., 2014). Groundwater vulnerability is an e̶s̶t̶i̶m̶a̶t̶e̶ ̶o̶f̶ ̶t̶h̶e̶ ̶r̶e̶l̶a̶t̶i̶v̶e̶ ̶h̶a̶z̶a̶r̶d̶ ̶o̶f̶

57   g̶r̶o̶u̶n̶d̶w̶a̶t̶e̶r̶ ̶p̶o̶l̶l̶u̶t̶i̶o̶n̶ by a specific constituent. Vulnerability maps are commonly performed at

58   a sub-basin, basin, or regional scale. They are not normally applied for site-specific e̶s̶t̶i̶m̶a̶t̶e̶s̶

59   including zones smaller than a few tens of square kilometers (Baalousha, 2006;Tilahun and

60   Merkel, 2010). Different techniques have been presented to assess groundwater susceptibility

61   with great precision (Javadi et al., 2010;Javadi et al., 2011). Mostly, these methods including

62   analytic tools considered to relate groundwater contamination with land operations. There are

63   three types of evaluation methods i̶n̶c̶l̶u̶d̶e̶; the overlay and index, the process-based simulation

64   and, the statistic procedures (Neshat et al., 2014;Dixon, 2004).

65   Overlay and index procedures affirm the incorporation of various zonal maps by allocating

66   a numeral index. Both procedures are simple to use in the geographic information system,

67   especially on a zonal measure. Hence, these methods are the most famous procedures applied to

68   vulnerability estimation (Neshat et al., 2014). T̶h̶e̶ ̶m̶o̶s̶t̶ ̶e̶x̶t̶e̶n̶s̶i̶v̶e̶l̶y̶ ̶u̶t̶i̶l̶i̶z̶e̶d̶ ̶a̶m̶o̶n̶g̶ ̶t̶h̶e̶s̶e̶

69   m̶e̶t̶h̶o̶d̶s̶ ̶e̶n̶c̶o̶m̶p̶a̶s̶s̶ GODS (Ghazavi and Ebrahimi, 2015), IRISH (Daly and Drew, 1999), AVI

70   (Raju et al., 2014), and DRASTIC (Neshat et al., 2014;Baghapour et al., 2014;Baghapour et al.,

71   2016).

72   The DRASTIC index for the first time proposed by Aller et al (1985). It is considered one of

73   the best indexes for the vulnerability of groundwater. This method ignores the influences of

74   zonal properties. Thus, identical weights and rating values are utilized. In addition, this technique

75   does not apply a standard validation test for the aquifer. Therefore, several investigators

76   developed this index using various techniques (Neshat et al., 2014). The higher DRASTIC index

77   represents the greater contamination potential and inversely. After calculating, the DRASTIC

78   index should be possible to identify the zones that are more prone to pollution. This index only

79   provides a relative estimate and is not created to make a complete assessment (Baalousha, 2006).

80   Many studies have been conducted using DRASTIC index to estimate the groundwater

81   vulnerability in the world different regions (Jaseela et al., 2016;Zghibi et al., 2016;Kardan

82   Moghaddam et al., 2017;Kumar et al., 2016;Neshat and Pradhan, 2017;Souleymane and Tang,

83   2017;Ghosh and Kanchan, 2016;Saida et al., 2017), however, fewer studies have used the

84   CDRASTIC index for evaluation of the groundwater vulnerability (Baghapour et al.,

85   2016;Baghapour et al., 2014;Secunda et al., 1998;Jayasekera et al., 2011;Shirazi et al.,

86   2012;Jayasekera et al., 2008). Boughriba et al. (2010) utilized DRASTIC index in geographical

87   information system environment for an estimate of the vulnerability in the aquifer. They provide

88   the DRASTIC modified map prepared from total DRASTIC indexes and small monitoring

89   network maps inclusive two classes, high and medium. Then they integrated the map with the

90   land use map to provide the contamination potential map. They reported that the new obtained

91   map inclusive three various classes very high, medium, and high. Babiker et al. (2005) used the

92   DRASTIC index to determine prone points to contamination from human activities in the

93 aquifer. They reported that the western and eastern parts of aquifer fall in the high and medium

94 categories, respectively. The final aquifer vulnerability map represents that the high risk of

95 pollution is in the eastern part of aquifer due to agriculture activities. They also observed that the

96 factor, net recharge has the most effect on the aquifer vulnerability, followed by the soil media,

97 topography, the impact of the vadose zone, and hydraulic conductivity.

98 The water difficulties in Iran with a mean annual rainfall about one-third of the world annual

99 rainfall (Chitsazan and Akhtari, 2006;Modabberi et al., 2017) are critical and serious. Also,

100 diminution in these rare resources has deteriorated this condition. Groundwater is the only water

101 source in the Kerman province due to the lack of surface water. The evaluated aquifer in this

102 research located in the central part of Kerman province in Iran. Due to recent droughts, this

103 aquifer is placed under heavy pumping to irrigate crops, which cause gradually reduces the water

104 level. Moreover, recently, the use of groundwater resources has been greater than in former

105 years. It causes the researches on the pathology and zoning the losses in groundwater undeniable.

106 Therefore, the purpose of this research is providing the Kerman–Baghin aquifer vulnerability

107 maps and performing the sensitivity analysis to identify the most effective factors in the

108 vulnerability.

109 **2. Methodology**

110 **2.1. Study area**

111 The Kerman Province covers both semiarid and waterless areas. The present study included a

112 2023 km^2 area (29° 47′ to 30° 31′ N latitude and 56° 18′ to 57° 37′ E longitude) located in the

113 central part of the Kerman Province, Iran (Figure 1). The study area is mostly covered by

114 agricultural land (Neshat et al., 2014). The mean annual rainfall in the study area is 108.3 mm (in

115 2017). The highest and lowest ground elevation in the study area is 1,980 and 1,633 m above sea

116   level, respectively. The mean, minimum, and maximum annual temperatures in the study area

117   are 17°C, -12°C, and 41°C, respectively (in 2017).
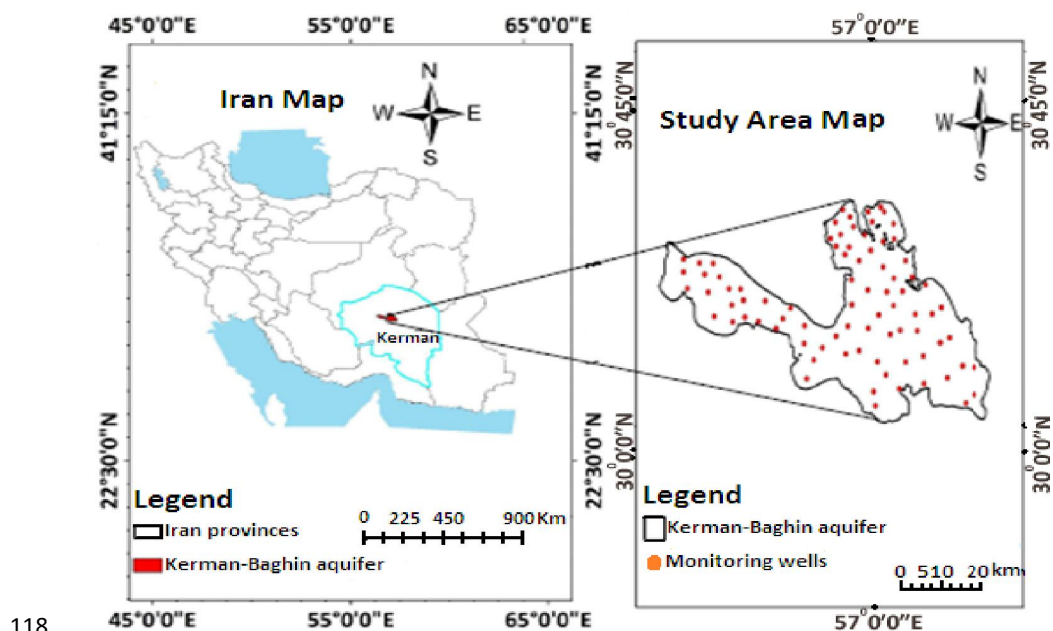
119   **Fig. 1.** Location map of the Kerman–Baghin aquifer

120   **2.2. Computing the DRASTIC and CDRASTIC indexes**

121   DRASTIC is a procedure developed by the United States Environmental Protection Agency (U.S

122   EPA) to prepare a systematic estimate of the potential for groundwater pollution (Aller et al.,

123   1985). Through this method, the DRASTIC index is obtained from the sum of the multiplication

124   of the rank and weight of the parameters. Higher sum values demonstrate greater vulnerability of

125   the aquifer to pollution. Vulnerability ranges corresponding to the DRASTIC index are presented

126   in Table. In the DRASTIC index, each parameter is rated on a scale from 1 to 10 that shows the

127   relative contamination potential of that parameter for that area. Also, in the DRASTIC index, one

128   weight is assigned to each of the parameters (1 to 5). Weight values show the relative

129   significance of the parameters with respect to each other. The DRASTIC index is obtained using

130   the following formula (Kardan Moghaddam et al., 2017;Neshat and Pradhan, 2017):

131    $$DRASTIC\ index = D_r D_W + R_r R_W + A_r A_w + S_r S_w + T_r T_w + I_r I_w + C_r C_W. \tag{1}$$

132   In the above formula, the letters in the acronym DRASTIC comprise a short form of the effective

133   factors in the DRASTIC index. Also, "r" and "w" are the rating and weight of each factor,

134   respectively. The ratings and weights of the factors are depicted in Table 2.

135   **Table 1** The range of vulnerability related to the DRASTIC index

Vulnerability	Ranges
Very low	23-46
Low	47-92
Moderate	93-136
High	137-184
Very high	>185

136

137   **Table 2** Rating and weight related to DRASTIC index factors

DRASTIC parameters	Range	Rating (r)	Weight (w)
Water table depth (m)	0.0-1.5	10	
	1.5-4.6	9	
	4.6-9.1	7	
	9.1-15.2	5	5
	15.2-22.9	3	
	22.9-30.5	2	
	>30.5	1	
Aquifer media	Rubble and sand	9	
	Gravel and sand	7	
	Gravel, sand, clay and silt	5	3
	Sand and clay	4	
	Sand, clay and silt	3	
Soil media	Rubble, sand, clay and silt	9	
	Gravel and sand	7	
	Gravel, sand, clay and silt	6	
	Sand	5	2
	Sand, clay and silt	3	
	clay and silt	2	

Topography or slope (%)	0-2	10	
	2-6	9	
	6-12	5	1
	12-18	3	
	>18	1	
The impact of the vadose zone	Rubble, sand, clay and silt	9	
	Gravel and sand	7	
	Gravel, sand, clay and silt	5	5
	Sand, clay and silt	3	
Hydraulic conductivity (m/day)	0-4.1	1	
	4.1-12.2	2	3
	12.2-28.5	4	
	28.5-40.7	6	
	40.7-81.5	8	

138

139 To get the CDRASTIC index, an additional factor (land use) is added to the above formula.

140 Thus, the CDRASTIC index was obtained as follows:

141 $\quad$ CDRASTIC index $= D_r D_W + R_r R_W + A_r A_w + S_r S_w + T_r T_w + I_r I_w + C_r C_W + L_r L_W.$ $\quad$ (2)

142 In the above formula, L_w and L_r are the relative weight and rating related to the land use factor,

143 respectively. Ratings and weightings applied to the pollution potential, which are related to the land

144 use factor based on the CDRASTIC index, are indicated in Table 3. The output of the CDRASTIC

145 index should be within the range of 28 to 280. Vulnerability ranges based on the CDRASTIC index

146 are presented in Table 4.

147 **Table 3** Ratings and weighting applied to the pollution potential related to the land use factor

148 based on the CDRASTIC index

Land use	Rating	Weight
Irrigated field crops + Urban areas	10	
Irrigated field crops + Grassland with poor vegetation cover + Urban areas	9	
Irrigated field crops + Grassland with moderate vegetation cover + Urban areas	8	
Irrigated field crops	8	
Irrigated field crops + Fallow land + Grassland with poor vegetation cover	7	
Irrigated field crops + Grassland with poor vegetation cover	7	
Irrigated field crops + Grassland with moderate vegetation cover	6	
Irrigated field crops + Rocky + Urban areas	5	5

Irrigated field crops + Grassland with poor vegetation cover + Woodland	5
Irrigated field crops + Woodland	5
Irrigated field crops + Rocky	4
Fallow land	3
Fallow land + Grassland with poor vegetation cover	3
Fallow land + Grassland with moderate vegetation cover	3
Grassland with poor vegetation cover	2
Grassland with moderate vegetation cover	2
Grassland with moderate vegetation cover + Woodland	1
Sand dune +Grassland with moderate vegetation cover	1
Sand dune	1

149

150   **Table 4** Vulnerability ranges related to the CDRASTIC index

Vulnerability	Ranges
Very low	<100
Low	100-145
Moderate	145-190
High	190-235
Very high	≥235

151   **2.3. Water table depth**

152   The water table depth factor is the ~~depth from the~~ Earth's surface ~~to the water table~~ in a well

153   (Baghapour et al., 2016). ~~To obtain this factor from existing information,~~ 83 wells in the

154   Kerman–Baghin aquifer were utilized. The interpolation procedure was used to provide a raster

155   map of the water table depth factor, which was categorized based on Table 2.

156   **2.4. Net recharge**

157   Net recharge is the amount of runoff that permeates ~~to the Earth~~ and reaches the groundwater

158   surface (Singh et al., 2015;Ghosh and Kanchan, 2016). This research uses the Piscopo method

159   (Chitsazan and Akhtari, 2009) to provide the net recharge layer for the Kerman–Baghin aquifer

160   according to the following equation and Table 5:

161   Net recharge factor = slope (%) + rainfall + soil permeability.   (3)

162   In the above equation, the percentage of slope was calculated from a digital elevation model,

163   ~~which was obtained from a topographical map~~. Also, a soil permeability map was created using

164   the Kerman–Baghin aquifer soil map (with scale 1:250000) and the drilling logs of the wells

165   ~~(number of wells: 83)~~. In the end, a map of ~~the area's~~ rainfall rate was compiled based on the

166   annual average precipitation. Ratings and weights of the net recharge factor are illustrated in

167   Table 5.

168   **Table 5** Weight, rating, and range of the net recharge parameter

Slope (%)		Rainfall		Soil permeability		Net Recharge		
Range (%)	Factor	Range (mm/year)	Factor	Range	Factor	Range (cm/year)	Rating	Weight
<2	4	>850	4	High	5	11-13	10	
2-10	3	700-850	3	Moderate to high	4	9-11	8	
10-33	2	500-700	2	Moderate	3	7-9	5	4
>33	1	<500	1	Low	2	5-7	3	
				Very low	1	3-5	1	

169   **2.5. Aquifer media**

170   ~~This~~ parameter controls the path of groundwater streams in the aquifer (Aller et al., 1985;Singh

171   et al., 2015). To obtain this layer, the well's drilling log data ~~(number of wells: 83) in the aquifer~~

172   were used. The data were gathered from the Kerman Regional Water Office (KRWO). The range

173   of the aquifer media layer is shown in Table 2.

174   **2.6. Soil media**

175   The soil media has a considerable effect on the amount of water surface that can penetrate into

176   the aquifer. Therefore, where the soil layer is thick, the debilitation processes such as absorption,

177   filtration, degradation, and evaporation may be considerable (Singh et al., 2015). A soil media

178   raster map was provided using the Kerman–Baghin aquifer soil map and the well's drilling logs.

Natural Hazards
and Earth System
2.7. Topography

The topography controls the ~~duration~~ of water ~~remaining~~ on the soil ~~surface~~ and the degree of penetration (Singh et al., 2015). For obtain this layer, the percentage of the slope was provided from a digital elevation model~~, which was obtained from the topographical map~~. The data were gathered from the KRWO. The range of the topographic layer is presented in Table 2.

2.8. The impact of the vadose zone

The vadose zone is ~~outlined as the area above the groundwater level which is unsaturated~~ (Singh et al., 2015). ~~This layer~~ plays a considerable role in decreasing groundwater contamination by pollutant debilitation processes such as purification, chemical reaction, and dispersal (Shirazi et al., 2012). In order to prepare this layer, ~~from~~ the wells drilling log data ~~(number of wells: 83) in the aquifer~~ were used. The data were gathered from the KRWO. The range ~~of the impact~~ of the vadose zone layer is depicted in Table 2.

2.9. Hydraulic conductivity

The hydraulic conductivity refers to the capability of aquifer ~~matters~~ to transfer water. The high hydraulic conductivity areas demonstrate a high potential for groundwater contamination (Singh et al., 2015;Aller et al., 1985). To prepare this layer, pumping tests ~~of wells~~ were used ~~(number of wells: 83)~~. The range of the hydraulic conductivity layer is shown in Table 2.

2.10. Land use

Groundwater is drastically connected with the perspective and land use that it underlies. Land use influences groundwater resources via variation in recharge and by changing demands ~~for water. Land use is obligatory since it is required by the CDRASTIC index.~~ The Indian remote

200   sensing satellite information was utilized to providing land use raster map. The weight and rating

201   related to the land use layer are presented in Table 3.

2.11. Sensitivity Analyses

203   One of the main advantages of the DRASTIC index is the ~~performance of evaluation using a~~

204   ~~more number of input data which can restrict the effects of errors or mistakes~~ on the final results.

205   Nevertheless, some investigators, like Babiker et al. (2005), Barber et al. (1993), and Merchant

206   (1994), reported that ~~we could obtain~~ similar results using fewer data and lower costs. The

207   unavoidable subjectivity related to the choice of the seven factors, ranks, and weights utilized to

208   calculate the vulnerability index has also been criticized. Therefore, in order to eliminate the

209   aforementioned criticisms, two sensitivity analyses were performed as follows (Napolitano and

210   Fabbri, 1996):

A. MRSA

212   MRSA value indicates the sensibility ~~of the vulnerability map~~ to ~~eliminating~~ one or more maps

213   from the suitability analysis. MRSA is calculated as follows (Babiker et al., 2005;Martínez-

214   Bastida et al., 2010;Saidi et al., 2011;Modabberi et al., 2017):

$$S = \left[\left| \frac{\frac{V}{N} - \frac{V'}{n}}{V} \right| \right] \times 100 \tag{4}$$

216   ~~In this formula,~~ S is the sensibility value expressed in terms of variation index, V is the intrinsic

217   vulnerability index (real vulnerability index) ~~index~~ and V′ is the intrinsic vulnerability index

218   after removal of factor X, N and n are the numbers of data factors utilized to calculate V and V′,

219   respectively (Babiker et al., 2005;Martínez-Bastida et al., 2010;Saidi et al., 2011;Modabberi et

220   al., 2017).

B. SPSA

221

222 SPSA was presented by Napolitano and Fabbri (1996) for the first time. This test shows the

223 effect of each of the DRASTIC factors in the final vulnerability index. Using this test derived

224 from equation 5, the real and effective weight of each factor compared to the theoretical weight

225 assigned by the analytical model (Babiker et al., 2005;Martínez-Bastida et al., 2010;Saidi et al.,

226 2011;Modabberi et al., 2017).

227
$$W = \left[\frac{P_r P_w}{V}\right] \times 100 \qquad (5)$$

228 In this above equation, W is the effective weight of each factor. P_r and P_w are the rank and

229 weight assigned to factor P, respectively. V is the intrinsic vulnerability index (Martínez-Bastida

230 et al., 2010;Babiker et al., 2005;Saidi et al., 2011;Modabberi et al., 2017).

231 **3. Results and discussion**

232 **3.1. DRASTIC and CDRASTIC parameters**

233 Based on the data shown in Table 2, the assigned rating of water table depth varies from 1 to 10.

234 In addition, based on the results presented in Table 6, the water table depth in the aquifer varies

235 from 4.6 to >30.5 m (rating 1 to 7). Around 27.55% of the aquifer has a depth of >30.5 m, and

236 66.16 % of the aquifer has a depth between 9.1 m and 30.5 m. Less than 7% has a depth between

237 4.6 m and 9.1 m. The Kerman–Baghin aquifer rated map of water table depth factor is presented

238 in Figure 2(A). According to Figure 2(A) and Table 6, the least impact of the water table depth

239 parameter on aquifer vulnerability occurs in parts of the center (6.39%), whereas the water table

240 depth parameter most influences vulnerability in parts of the north, south, northwest, and

241 southeast (27.55%).

242   According to the results presented in Table 6, 75.81% of the aquifer has a net recharge value

243   in the range of 7 to 9 cm/year. The highest rating of 8 is dedicated only to 11.74% of the aquifer

244   that has a net recharge value between 9 and 11 cm/year. The Kerman–Baghin aquifer rated map

245   of the net recharge parameter is shown in Figure 2(B). According to Piscopo's method, the

246   Kerman–Baghin aquifer was divided into three classes with regards to the net recharge factor.

247   The highest net recharge value was seen in the north, northeast, south, southwest, parts of the

248   northwest, parts of the center, and parts of the southeast (75.81%), whereas the least net recharge

249   value appeared in parts of the northwest and center (11.74%), as shown in Figure 2(B) and Table

250   6.

251   As observed in Table 6, the majority of the Kerman–Baghin aquifer media is composed of

252   sand, clay, and silt (75.21%). The Kerman–Baghin aquifer rated map of aquifer media is

253   presented in Figure 3(A). Parts of the aquifer in the north, northwest, northeast, center, and

254   southeast are composed of sand, clay, and silt. Parts of the aquifer in the northwest are composed

255   of rubble and sand (5.58%). Parts of the aquifer in the south and northwest are composed of

256   gravel and sand (8.95%), and gravel, sand, clay, and silt (10.26%).

257   The Kerman–Baghin aquifer rated map of the soil media parameter is presented in Figure

258   3(B). The soil map depicts six different classes of the soil. The highest rank (rank = 9) was

259   assigned to rubble, sand, clay, and silt (a combination of rubble, sand, clay and silt soils). Also,

260   the lowest rank (rank = 2) was assigned to clay and silt (a combination of clay and silt soils).

261   Most of the aquifer soil media is covered with silt, sand, and clay (about 80%).

262   The Kerman–Baghin aquifer rated map of the topography parameter is indicated in Figure

263   4(A). The topographical layer shows a gentle slope (0 to 6%) over most of the aquifer, hence

264   gaining ranks of 9 and 10. A slope range of 0 to 2% includes 34.72% of the study area, and its

265   rating (slope range = 0–2%) is 10. A rank of 9 is dedicated for 65.28% of the aquifer, which has

266   a 2 to 6% slope (parts of the northwest) as shown in Figure 4(A) and Tables 2 and 6. As the

267   gradient increases, the runoff increases as well (Israil et al., 2006) leading to less penetration

268   (Jaiswal et al., 2003). Based on Madrucci et al.'s study (2008), the gradients higher than 35° are

269   considered restrictions on groundwater desirability because of the lack of springs.

270   The Kerman–Baghin aquifer rated map of the impact of the vadose zone parameter is

271   indicated in Figure 4(B). According to the results, the soil with a rank of 5 (gravel, sand, clay,

272   and silt) is more effective on aquifer vulnerability (35.47%). Other various types of soils such as

273   sand, clay, and silt (parts of the north, northeast, south, and southeast), gravel and sand (parts of

274   the center and northwest), and rubble, sand, clay, and silt (parts of the northwest) cover 34.24%,

275   20.39%, and 9.9% of the aquifer, respectively, as shown in Figure 4(B) and Table 6. Sandy soil

276   is effective on groundwater occurrence because of the high rate of penetration (Srivastava and

277   Bhattacharya, 2006). However, clay soil is arranged poorly because of the low infiltration

278   (Manap et al., 2014b).

279   The Kerman–Baghin aquifer rated map of the hydraulic conductivity parameter is presented

280   in Figure 5(A). The hydraulic conductivity factor shows high variability. Our study results show

281   that the hydraulic conductivity parameter of the Kerman–Baghin aquifer varied from 0 to 81.5

282   m/day. The potential for groundwater contamination is more for zones with high hydraulic

283   conductivity (38.27%). As shown in Figure 5(A) and Table 6, 29.51%, 23.93%, 5.98%, and

284   2.31% of the study areas have hydraulic conductivity in the ranges of 0 to 4.1 m/day, 12.2 to

285   28.5 m/day, 28.5 to 40.7 m/day, and 40.7 to 81.5 m/day, respectively.

286   The Kerman–Baghin aquifer rated map of the land use parameter is presented in Figure 5(B).

287   Our results show that the majority of the Kerman–Baghin aquifer is covered with irrigated field

288 crops and grassland with moderate vegetation cover (20.45%). Less than 4% ~~of land use~~ of the

289 study area is irrigated field crops and urban areas (3.61%), and 58.47% ~~of land use~~ of the study

290 area is irrigated field crops with urban areas, grassland with poor and moderate vegetation cover,

291 fallow land, woodland, and rocky ground. In addition, 10.17% ~~of land use~~ of the study area is

292 fallow land with poor grassland and moderate vegetation cover, and 13.72% ~~of land use~~ of the

293 study area is sand dunes with poor grassland and moderate vegetation cover and woodland as

294 shown in Figure 5(B) and Tables 3 and 6.
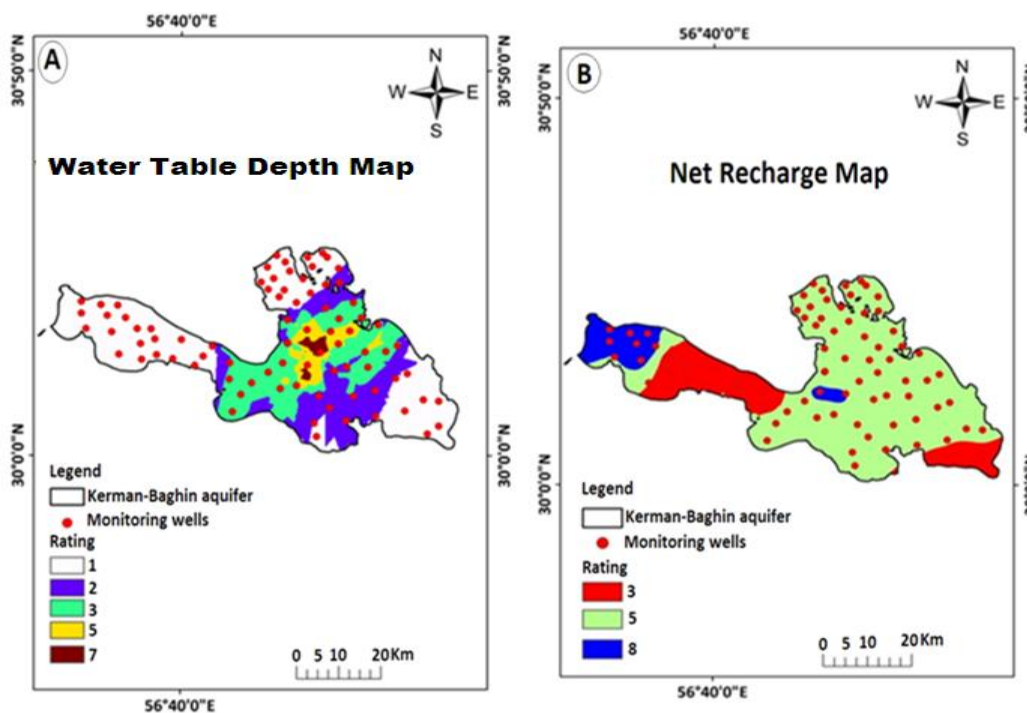
295

296 **Fig. 2.** Kerman–Baghin aquifer rated maps of A) water table depth and B) net recharge
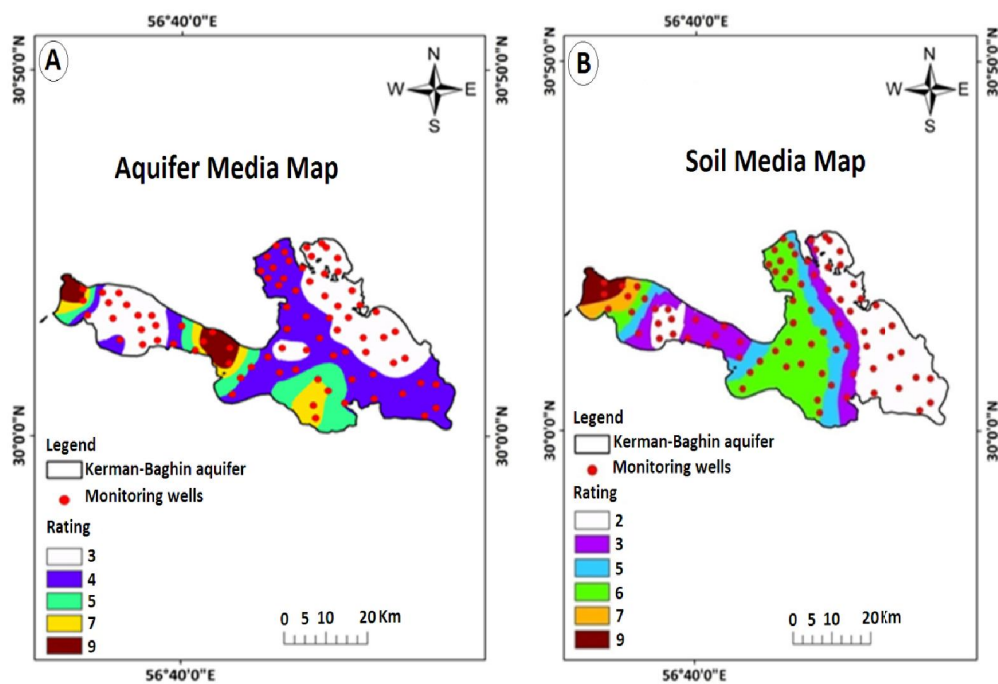
297

298 **Fig. 3.** Kerman–Baghin aquifer rated maps of A) aquifer media and B) soil media
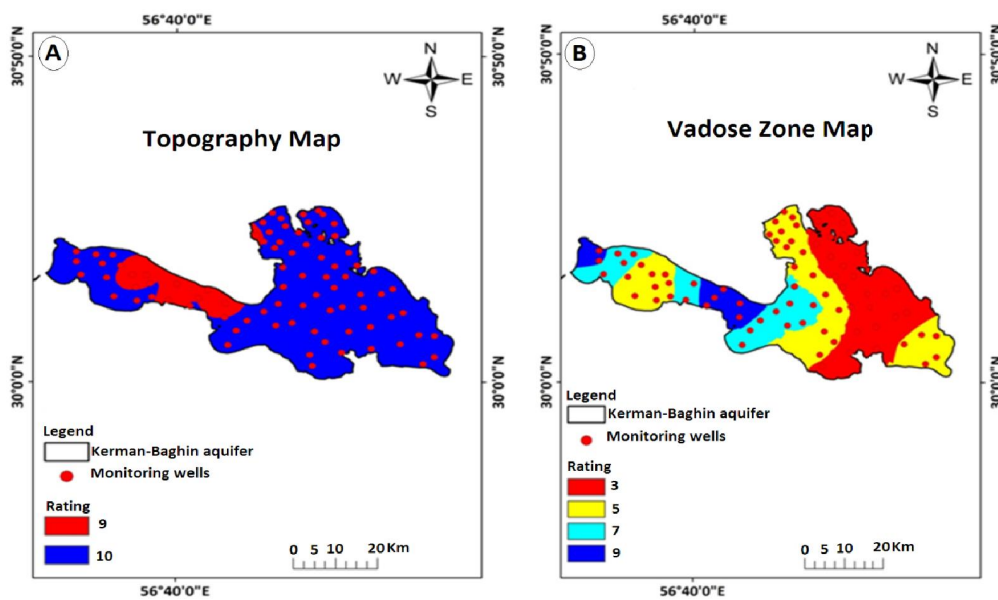
299

300 **Fig. 4.** Kerman–Baghin aquifer rated maps of A) topography and B) vadose zone
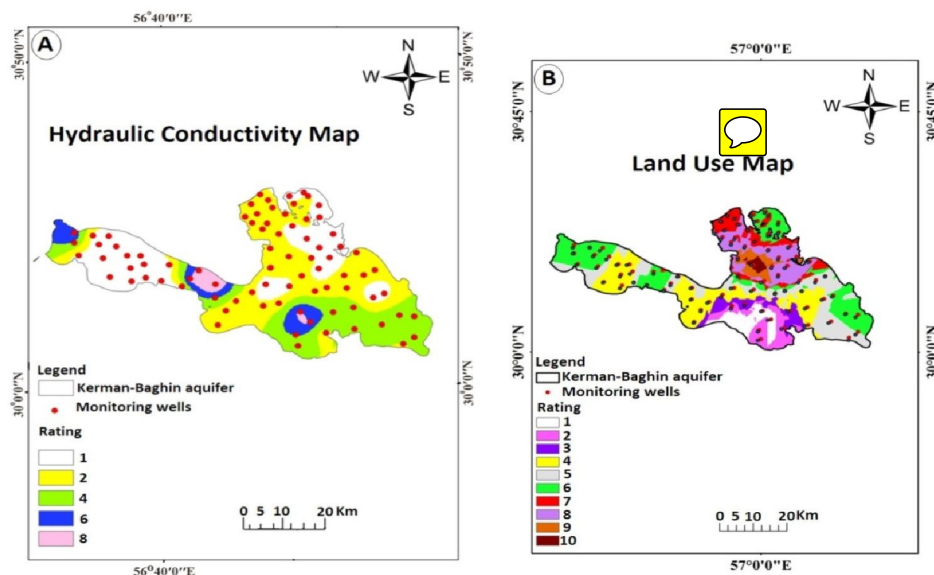
301

302   **Fig. 5.** Kerman–Baghin aquifer rated maps of A) hydraulic conductivity and B) land use

303   **Table 6** The area of rating (km^2 and %) of the DRASTIC and CDRASTIC parameters

DRASTIC and CDRASTIC indexes parameters	Rating	Area (km^2)	Area (%)	The aquifer geographic directions covered by the respective rating in the parameters rated maps
Water table depth	1	557.73	27.55	Parts of the north, south, northwest, and southeast
	2	472.18	23.34	Parts of the north south, and center
	3	469.78	23.29	Parts of the center
	5	395.00	19.53	Parts of the center
	7	129.14	6.39	Parts of the center
Net recharge	3	252.04	12.45	Parts of southeast, and northwest
	5	1534.15	75.81	North, northeast, south, southwest, and parts of the northwest, center, southeast
	8	237.6	11.74	Parts of the northwest and center
Aquifer media	3	743.18	36.72	Parts of the north, northwest, northeast, and center
	4	779.01	38.49	Parts of the north, northwest, southeast, and center
	5	207.81	10.26	Parts of the south, and northwest
	7	181.02	8.95	Parts of the south, and northwest
	9	112.76	5.58	Parts of the northwest
Soil media	2	658.5	32.53	Parts of the north, northwest, northeast, and southeast
	3	399.72	19.75	Parts of the north, northwest, south, and center

	5	297.44	14.69	Parts of the north, northwest, south, and center
	6	538.77	26.62	Parts of the northwest, center, and southwest
	7	67.56	3.33	Parts of the northwest
	9	61.79	3.08	Parts of the northwest
Topography	9	702.74	34.72	North, northwest, northeast, south, southeast, southwest, and center
	10	1321.07	65.28	parts of the northwest
The impact of the vadose zone	3	692.87	34.24	Parts of the north, northeast, south, and southeast
	5	717.91	35.47	Parts of the north, northwest, south, southeast, and center
	7	412.49	20.39	Parts of the center, and northwest
	9	200.53	9.9	Parts of the northwest
Hydraulic conductivity	1	597.11	29.51	Parts of the northeast, northwest, southeast, and center
	2	774.52	38.27	parts of the northwest, south, southeast and center
	4	484.17	23.93	Parts of the northwest, south, and southeast
	6	120.99	5.98	Parts of the south, and northwest
	8	46.7	2.31	Parts of the south, and northwest
Land use	1	112.48	5.56	Parts of the south
	2	165.02	8.16	Parts of the south
	3	205.65	10.17	Parts of the south, and center
	4	357.06	17.64	Parts of the south, southwest, northwest and center
	5	234.86	11.61	Parts of the southeast, northwest, and center
	6	413.86	20.45	Parts of the southeast, northwest, northeast, and center
	7	182.63	9.02	Parts of the north, northwest, and northeast
	8	169.4	8.37	Parts of the north, northwest, and northeast
	9	109.42	5.41	Parts of the north, northwest, and northeast
	10	73.09	3.61	Parts of the north

3.2. DRASTIC and CDRASTIC vulnerability indexes

304

305 The Kerman–Baghin aquifer vulnerability map using DRASTIC and CDRASTIC indexes is

306 shown in Figure 6. In the studied aquifer, the vulnerability falls under very high, high, moderate,

307 very low, and low vulnerable areas. It is found that in both indexes, the parts of north, northeast,

308 northwest, south, southwest, southeast and center come under low and very low vulnerability.

309 This can be attributed to low water depth, hydraulic conductivity, and net recharge in these

310   aquifer areas ~~and the~~ other reason might be that the aquifer media ~~mostly~~ are clay, sand and silt

311   soils. The area of the vulnerability identified by investigated indexes is illustrated in Table 7.

312   Low and very low vulnerable zones cover 25.21% and 38.31% of the Kerman–Baghin aquifer

313   using the DRASTIC index~~, respectively~~. Very low and low vulnerable zones cover 24.95% and

314   40.41% ~~of the Kerman Baghin aquifer~~ using the CDRASTIC index~~, respectively~~. This is

315   primarily due to water depth and relatively low permeability of the vadose zone in such aquifers

316   (Colins et al., 2016). Around 26 % of the studied aquifer ~~area~~ has moderate groundwater

317   pollution potential using DRASTIC and CDRASTIC indexes. This does not mean that such areas

318   are without pollution but it is relatively prone to pollution when compared with other areas

319   (Colins et al., 2016). From the DRASTIC index values, it was noticed that 10.4% of the study

320   aquifer is under high (8.46%) and very high (1.94%) ~~of~~ vulnerability. The results of the study

321   showed that 8.75% of the aquifer is under high (6.28%) and very high (2.47%) ~~of~~ vulnerability in

322   the CDRASTIC index. The vulnerability maps according to these two indexes indicated very

323   same findings, showing the northwest portion of the aquifer as the high and very high vulnerable

324   zones. The ~~high~~ vulnerability can be attributed to high water depth, hydraulic conductivity, and

325   net recharge in these aquifer areas. In addition, this can due to the ~~high~~ slope in this area.

326
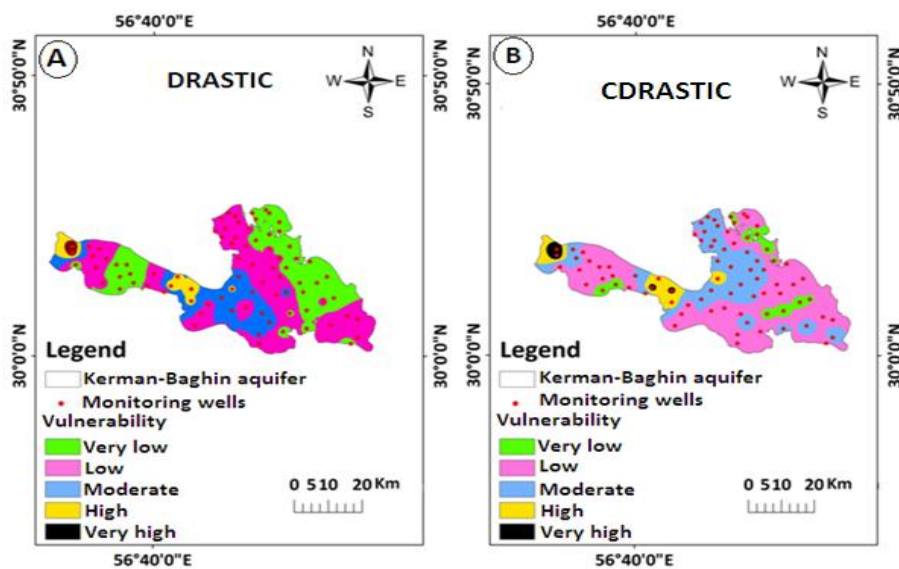
Fig. 6. The vulnerability maps of the Kerman–Baghin aquifer by DRASTIC and CDRASTIC

indexes

Table 7 The area of vulnerability (km^2 and %) identified by DRASTIC and CDRASTIC indexes

The sensibility of the DRASTIC index

Vulnerability	DRASTIC				composite DRASTIC			
	Ranges	Area (km^2)	Area (%)	The aquifer geographic directions covered by the respective vulnerability	Ranges	Area (km^2)	Area (%)	The aquifer geographic directions covered by the respective vulnerability
Very low	23-46	510.25	25.21	Parts of the south, north, northwest, and northeast	<100	505.02	24.95	Parts of the southeast, north, northwest, and northeast
Low	47-92	775.14	38.31	Parts of the south, southwest, southeast, north, northwest, northeast, and center	100-145	817.70	40.41	Parts of the south, southwest, southeast, north, northwest, northeast, and center
Moderate	93-136	527.85	26.08	Parts of the south, south west, northwest, and center	145-190	524.06	25.89	Parts of the south, southwest, southwest, northwest, and center
High	137-184	171.02	8.46	Parts of the northwest	190-235	126.91	6.28	Parts of the northwest and center
Very high	>185	39.23	1.94	Parts of the northwest	≥235	49.79	2.47	Parts of the northwest

331

3.3. Sensitivity of the DRASTIC model

333   The MRSA to the DRASTIC index is performed by eliminating one layer data at a time as

334   indicated in Table 8. The results showed a high variation in vulnerability index when the impact

335   of the vadose zone factor was removed, so that, the average variation index is 1.88%. This shows

336   that this factor is more effective in vulnerability assessment using the DRASTIC index. When

337   this parameter is removed from the overlay process, this leads to a significant decrease in

338   vulnerability index. This could be due to the high theoretical weight allocated to this factor

339   (weight = 5). These findings are similar to those obtained by Dibi et al. (2012) who have shown

340   that in addition to this parameter, topography, net recharge, and water table depth have a high

341   impact on the vulnerability index. Also, in Samake et al. (2011) study, the impact of the vadose

342   zone and the hydraulic conductivity parameters had a considerable impact on the vulnerability

343   index. The vulnerability index appears to have a moderate sensitivity to the deletion of water

344   table depth (1.48%), net recharge (1.36%), and hydraulic conductivity (1.25%) parameters. The

345   minimum menu variation index was achieved after eliminating the aquifer media factor (0.44%),

346   as indicated in Table 8.

347   For the estimate of the effect of individual factors towards aquifer vulnerability, the SPSA is

348   performed. The results summary of SPSA to the DRASTIC index is shown in Table 9. The

349   SPSA compares the effective weights and theoretical weights. The average value of the effective

350   weight of the net recharge factor is 43.26% and its theoretical weight (%) is 17.4%. This shows

351   that this factor is more effective in vulnerability assessment using the DRASTIC index. The

352   results reported by other studies (Babiker et al., 2005;Doumouya et al., 2012) are similar to those

353   of the present study. The impact of the vadose zone and water table depth parameters has high

354   theoretical weights (21.74%). They have been dedicated with an effective weight with average

355   value such as 8.33% and 25.55%. The remaining factors show an average value of the effective

356   weights of 14.91% (aquifer media), 9.89% (soil media), 11.35% (topography), and 7.01%

357   (hydraulic conductivity). The theoretical weights allocated to the water table depth, net recharge,

358   topography, and hydraulic conductivity parameters are not in agreement with the effective

359   weight. The highest and lowest impact on aquifer vulnerability was related to the net recharge

360   and hydraulic conductivity parameters, respectively (Table 9).

361   **Table 8** Statistical results of MRSA in the DRASTIC index

Sensitivity of variability index (S) (%)				Removed parameters
SD	Min.	Max.	Ave.	
0.414	0.05	2.36	1.36	D
0.775	0.07	3.06	1.48	R
0.311	0.05	1.31	0.44	A
0.486	0.00	1.65	0.73	S
0.339	0.03	1.31	0.51	T
0.894	0.25	3.84	1.88	I
0.550	0.03	1.98	1.25	C

362

363   **Table 9** Statistical results of SPSA in the DRASTIC index

Effective weight (%)				Theoretical weight (%)	Theoretical weight	Parameters
SD	Min.	Max.	Ave.			
6.179	3.23	28.46	8.33	21.74	5	D
11.998	14.06	73.47	43.26	17.4	4	R
3.190	7.26	22.13	14.91	13.04	3	A
2.916	4.49	14.29	9. 89	8.7	2	S
2.222	6.45	14.71	11.35	4.3	1	T
5.367	15.79	37.31	25.55	21.74	5	I
3.738	2.42	18.75	7.01	13.04	3	C

364

365   **3.4. The sensibility of the CDRASTIC index**

366   The MRSA to the CDRASTIC index is performed by eliminating on data layer at a time as

367   indicated in Table 10. The mean variation index of hydraulic conductivity parameter is 4.13%.

368   The hydraulic conductivity has a greater effect in the aquifer vulnerability followed by water

369   table depth (4.05%), soil media (3.82%), topography (3.68%), aquifer media (3.28%), net

370   recharge (2.72%), the impact of the vadose zone (2.33%), and land use parameter (1.99%).

371   The effective weight derived from the SPSA to the CDRASTIC index is shown in Table 11.

372   The average value of the effective weight of the net recharge factor is 32.62%. This shows that

373   this factor is more effective in vulnerability assessment using CDRASTIC index. The hydraulic

374   conductivity displays the lowest effective weights (5.32%). The topography, net recharge, and

375   land use had upper effective weights toward the theoretical weights specified by CDRASTIC

376   index. The average value of the effective weight of the land use parameter is 24.82%. This shows

377   that this parameter is the second effective parameter in aquifer vulnerability using the

378   CDRASTIC index (Table 11).

379   **Table 10** Statistical results of MRSA in the CDRASTIC index

Sensitivity of variability index (S) (%)				Removed parameters
SD	Min.	Max.	Ave.	
1.403	0.50	6.48	4.05	D
1.617	0.11	10.91	2.72	R
1.541	0.06	5.99	3.28	A
1.508	0.67	6.60	3.82	S
1.353	0.87	5.87	3.68	T
1.439	0.06	5.12	2.33	I
1.480	0.55	6.72	4.13	C
0.375	1.23	3.00	1.99	L

380

381   **Table 11** Statistical results of SPSA in the CDRASTIC index

Effective weight (%)				Theoretical weight (%)	Theoretical weight	Parameters
SD	Min.	Max.	Ave.			
4.849	2.63	26.88	6.27	21.74	5	D
10.672	10.4	66.67	32.62	17.4	4	R
3.026	6.29	20.00	11.23	13.04	3	A
2.621	3.31	12.96	7.5	8.7	2	S
1.609	5.2	12.82	8.45	4.3	1	T
4.648	10.87	32.05	19.2	21.74	5	I
3.134	2.1	14. 88	5.32	13.04	3	C
10.122	3.88	42.37	24.82	17.85	5	L

382

383   **4. Conclusions**

384   Evaluations of vulnerability indexes for the Kerman–Baghin aquifer were conducted using the

385   GIS-based DRASTIC and CDRASTIC indexes. Seven hydro–geological factors (the letters

386   comprising the acronym) are applied to determine vulnerability with DRASTIC. ~~Eight~~ hydro–

387   geological parameters (one additional to the seven in DRASTIC) ~~are utilized to determine~~

388   ~~vulnerability~~ with the CDRASTIC index. From the DRASTIC index values, it was determined

389   that 10.4% of the aquifer is under high (8.46%) and very high (1.94%) vulnerability. From the

390   CDRASTIC index values, it was determined that 8.75% of the aquifer is under high (6.28%) and

391   very high (2.47%) vulnerability. Also, we found that parts of the north, south, southeast, and

392   northwest are under low and very low vulnerability using the DRASTIC and CDRASTIC

393   indexes. Agricultural and industrial activities are found to be a major threat in the zones with

394   high and very high vulnerability. The MRSA signifies the fact that hydraulic conductivity and

395   the impact of the vadose zone factors induce a high risk of aquifer contamination according to

396   the DRASTIC and CDRASTIC indexes, respectively. In both indexes, the SPSA analysis shows

397   the net recharge factor as a high risk for aquifer contamination. These results indicate that the

398   studied indexes are effective tools for determining groundwater vulnerability. Also, these results

399   could be utilized by private and government agencies as a guide for groundwater contamination

400   assessment in Iran.

401   **Acknowledgments**

402   The authors would like to thank the Environmental Health Engineering Research Center,

403   Kerman University of Medical Sciences, for their scientific support.

404   **Competing interests.** The authors declare that they have no conflict of interest.

405   **References**

406   Aller, L., Truman, b., Jay H, L., Rebeeca J, P., and Glen, H.: DRASTIC: a standardized system

407   for evaluating ground water pollution potential using hydrogeologic settings, U.S Environmental

408   Protection Agency, USA, 1985.

409   Ayazi, M. H., Pirasteh, S., Arvin, A., Pradhan, B., Nikouravan, B., and Mansor, S.: Disasters and

410   risk reduction in groundwater: Zagros Mountain Southwest Iran using geoinformatics

411   techniques, Disaster Adv., 3, 51-57, 2010.

412   Baalousha, H.: Vulnerability assessment for the Gaza Strip, Palestine using DRASTIC, J.

413   Environ. Geol., 50, 405-414, https://doi.org/10.1007/s00254-006-0219-z, 2006.

414   Babiker, I. S., Mohamed, M. A., Hiyama, T., and Kato, K.: A GIS-based DRASTIC model for

415   assessing aquifer vulnerability in Kakamigahara Heights, Gifu Prefecture, central Japan, Sci

416   Total Environ., 345, 127-140, https://doi.org/10.1016/j.scitotenv.2004.11.005, 2005.

417   Baghapour, M. A., Talebbeydokhti, N., Tabatabee, H., and Nobandegani, A. F.: Assessment of

418   groundwater nitrate pollution and determination of groundwater protection zones using

419   DRASTIC and composite DRASTIC (CD) models: the case of Shiraz unconfined aquifer, J.

420   Health. Sci. Surveill. Syst., 2, 54-65, 2014.

421   Baghapour, M. A., Nobandegani, A. F., Talebbeydokhti, N., Bagherzadeh, S., Nadiri, A. A.,

422   Gharekhani, M., and Chitsazan, N.: Optimization of DRASTIC method by artificial neural

423   network, nitrate vulnerability index, and composite DRASTIC models to assess groundwater

424   vulnerability for unconfined aquifer of Shiraz Plain, Iran, J Environ Health Sci Eng., 14, 1-16,

425   https://doi.org/10.1186/s40201-016-0254-y, 2016.

426   Barber, C., Bates, L. E., Barron, R., and Allison, H.: Assessment of the relative vulnerability of

427   groundwater to pollution: a review and background paper for the conference workshop on

428   vulnerability assessment, AGSO J Aust Geol Geophys., 14, 147-154, 1993.

429 Boughriba, M., Barkaoui, A.-e., Zarhloule, Y., Lahmer, Z., El Houadi, B., and Verdoya, M.:

430 Groundwater vulnerability and risk mapping of the Angad transboundary aquifer using

431 DRASTIC index method in GIS environment, Arab J Geosci., 3, 207-220,

432 https://doi.org/10.1007/s12517-009-0072-y, 2010.

433 Chitsazan, M., and Akhtari, Y.: Evaluating the potential of groundwater pollution in Kherran and

434 Zoweircherry plains through GIS-based DRASTIC model, J. Water. Wastewater, 17, 39-51,

435 2006.

436 Chitsazan, M., and Akhtari, Y.: A GIS-based DRASTIC model for assessing aquifer

437 vulnerability in Kherran Plain, Khuzestan, Iran, Water Resour Manag., 23, 1137-1155,

438 https://doi.org/10.1007/s11269-008-9319-8, 2009.

439 Colins, J., Sashikkumar, M., Anas, P., and Kirubakaran, M.: GIS-based assessment of aquifer

440 vulnerability using DRASTIC Model: A case study on Kodaganar basin, Earth Sci. Res. J., 20, 1-

441 8, https://doi.org/10.15446/esrj.v20n1.52469, 2016.

442 Daly, D., and Drew, D.: Irish methodologies for karst aquifer protection, in: Beek B (ed)

443 Hydrogeology and engineering geology of sinkholes and karst, Balkema, Rotterdam, 267-272,

444 1999.

445 Dibi, B., Kouame, K. I., Konan-Waidhet, A. B., Savane, I., Biemi, J., Nedeff, V., and Lazar, G.:

446 Impact of agriculture on the quality of groundwater resources in peri-urban zone of Songon

447 (Cote   D'ivoire),   Environ.   Engine.   Manage.   J.,   11,   2173-2182,

448 https://doi.org/10.30638/eemj.2012.271, 2012.

449 Dixon, B.: Prediction of ground water vulnerability using an integrated GIS-based Neuro-Fuzzy

450 techniques, J. Spat. Hydro., 4, 1-38, 2004.

451 Doumouya, I., Dibi, B., Kouame, K. I., Saley, B., Jourda, J. P., Savane, I., and Biemi, J.:

452 Modelling of favourable zones for the establishment of water points by geographical information

453 system (GIS) and multicriteria analysis (MCA) in the Aboisso area (South-east of Côte d'Ivoire),

454 Environ. Earth. Sci., 67, 1763-1780, https://doi.org/10.1007/s12665-012-1622-2, 2012.

455 Ghazavi, R., and Ebrahimi, Z.: Assessing groundwater vulnerability to contamination in an arid

456 environment using DRASTIC and GOD models, Inte. J. Environ. Sci. Tech, 12, 2909-2918,

457 https://doi.org/10.1007/s13762-015-0813-2, 2015.

458 Ghosh, T., and Kanchan, R.: Aquifer vulnerability assessment in the Bengal alluvial tract, India,

459 using GIS based DRASTIC model, Model Earth Syst Environ., 2, 2-13,

460 https://doi.org/10.1007/s40808-016-0208-5, 2016.

461 Israil, M., Al-hadithi, M., Singhal, D., Kumar, B., Rao, M. S., and Verma, S.: Groundwater

462 resources evaluation in the Piedmont zone of Himalaya, India, using Isotope and GIS techniques,

463 J. Spatial. Hydro., 6, 107-119, 2006.

464 Jaiswal, R., Mukherjee, S., Krishnamurthy, J., and Saxena, R.: Role of remote sensing and GIS

465 techniques for generation of groundwater prospect zones towards rural development--an

466 approach, Int J Remote Sens., 24, 993-1008, https://doi.org/10.1080/01431160210144543, 2003.

467 Jaseela, C., Prabhakar, K., and Harikumar, P. S. P.: Application of GIS and DRASTIC modeling

468 for evaluation of groundwater vulnerability near a solid waste disposal site, Int. J. Geoscien., 7,

469 558-571, https://doi.org/10.4236/ijg.2016.74043, 2016.

470 Javadi, S., Kavehkar, N., Mousavizadeh, M., and Mohammadi, K.: Modification of DRASTIC

471 model to map groundwater vulnerability to pollution using nitrate measurements in agricultural

472 areas, J. Agr. Sci. Tech., 13, 239-249, 2010.

473 Javadi, S., Kavehkar, N., Mohammadi, K., Khodadadi, A., and Kahawita, R.: Calibrating

474 DRASTIC using field measurements, sensitivity analysis and statistical methods to assess

475 groundwater vulnerability, Water. Int., 36, 719-732,

476 https://doi.org/10.1080/02508060.2011.610921, 2011.

477 Jayasekera, D., Kaluarachchi, J. J., and Villholth, K. G.: Groundwater Quality Impacts Due to

478 Population Growth and Land Use Exploitation in the Coastal Aquifers of Sri Lanka, Southern

479 Illinois University Carbondale 2008, 43,

480 Jayasekera, D. L., Kaluarachchi, J. J., and Villholth, K. G.: Groundwater stress and vulnerability

481 in rural coastal aquifers under competing demands: a case study from Sri Lanka, Environ Monit

482 Assess. , 176, 13-30, https://doi.org/10.1007/s10661-010-1563-8, 2011.

483 Kardan Moghaddam, H., Jafari, F., and Javadi, S.: Vulnerability evaluation of a coastal aquifer

484 via GALDIT model and comparison with DRASTIC index using quality parameters, Hydro. Sci.

485 J., 62, 137-146, https://doi.org/10.1080/02626667.2015.1080827, 2017.

486 Kumar, P., Thakur, P. K., Bansod, B. K., and Debnath, S. K.: Assessment of the effectiveness of

487 DRASTIC in predicting the vulnerability of groundwater to contamination: a case study from

488 Fatehgarh Sahib district in Punjab, India, Environ. Earth. Sci., 75, 879,

489 https://doi.org/10.1007/s12665-016-5712-4, 2016.

490 Madrucci, V., Taioli, F., and de Araújo, C. C.: Groundwater favorability map using GIS

491 multicriteria data analysis on crystalline terrain, Sao Paulo State, Brazil, J. Hydro., 357, 153-173,

492 https://doi.org/10.1016/j.jhydrol.2008.03.026, 2008.

493 Manap, M. A., Sulaiman, W. N. A., Ramli, M. F., Pradhan, B., and Surip, N.: A knowledge-

494 driven GIS modeling technique for groundwater potential mapping at the Upper Langat Basin,

495 Malaysia, Arabian. J. Geosci., 6, 1621-1637, https://doi.org/10.1007/s12517-011-0469-2, 2013.

496   Manap, M. A., Nampak, H., Pradhan, B., Lee, S., Sulaiman, W. N. A., and Ramli, M. F.:

497   Application of probabilistic-based frequency ratio model in groundwater potential mapping using

498   remote sensing data and GIS, Arabian. J.Geosci., 7, 711-724, https://doi.org/10.1007/s12517-

499   012-0795-z, 2014a.

500   Manap, M. A., Nampak, H., Pradhan, B., Lee, S., Sulaiman, W. N. A., and Ramli, M. F.:

501   Application of probabilistic-based frequency ratio model in groundwater potential mapping using

502   remote sensing data and GIS, Arabian. J. Geosci., 7, 711-724, https://doi.org/10.1007/s12517-

503   012-0795-z, 2014b.

504   Martínez-Bastida, J. J., Arauzo, M., and Valladolid, M.: Intrinsic and specific vulnerability of

505   groundwater in central Spain: the risk of nitrate pollution, Hydro. J., 18, 681-698,

506   https://doi.org/10.1007/s10040-009-0549-5, 2010.

507   Merchant, J. W.: GIS-based groundwater pollution hazard assessment: a critical review of the

508   DRASTIC model, Photogramm Eng Remote Sensing., 60, 1117-1127, 1994.

509   Modabberi, H., Hashemi, M. M. R., Ashournia, M., and Rahimipour, M. A.: Sensitivity Analysis

510   and Vulnerability Mapping of the Guilan Aquifer Using Drastic Method, Rev. Environ. Earth.

511   Sci., 4, 27-41, https://doi.org/10.18488/journal.80.2017.41.27.41, 2017.

512   Napolitano, P., and Fabbri, A.: Single-parameter sensitivity analysis for aquifer vulnerability

513   assessment using DRASTIC and SINTACS, Proceedings of the Vienna Conference,

514   Netherlands, 1996, 559-566,

515   Neshat, A., Pradhan, B., Pirasteh, S., and Shafri, H. Z. M.: Estimating groundwater vulnerability

516   to pollution using a modified DRASTIC model in the Kerman agricultural area, Iran, Environ.

517   Earth. Sci., 71, 3119-3131, https://doi.org/10.1007/s12665-013-2690-7, 2014.

518   Neshat, A., and Pradhan, B.: Evaluation of groundwater vulnerability to pollution using

519   DRASTIC framework and GIS, Arabian. J. Geosci., 10, 2-8, https://doi.org/10.1007/s12517-017-

520   3292-6, 2017.

521   Raju, N. J., Ram, P., and Gossel, W.: Evaluation of groundwater vulnerability in the lower

522   Varuna catchment area, Uttar Pradesh, India using AVI concept, J. Geol. Soc. India., 83, 273-

523   278, https://doi.org/10.1007/s12594-014-0039-9, 2014.

524   Saida, S., Tarik, H., Abdellah, A., Farid, H., and Hakim, B.: Assessment of groundwater

525   vulnerability to nitrate based on the optimised DRASTIC models in the GIS Environment (Case

526   of   Sidi   Rached   Basin,   Algeria),   Geosciences,   7,   2-23,

527   https://doi.org/10.3390/geosciences7020020, 2017.

528   Saidi, S., Bouri, S., and Ben Dhia, H.: Sensitivity analysis in groundwater vulnerability

529   assessment based on GIS in the Mahdia-Ksour Essaf aquifer, Tunisia: a validation study, Hydro.

530   Sci. J., 56, 288-304, https://doi.org/10.1080/02626667.2011.552886, 2011.

531   Samake, M., Tang, Z., Hlaing, W., Mbue, I. N., Kasereka, K., and Balogun, W. O.: Groundwater

532   vulnerability assessment in shallow aquifer in Linfen Basin, Shanxi Province, China using

533   DRASTIC model, J. Sustain. Develop., 4, 53-71, https://doi.org/10.5539/jsd.v4n1p53, 2011.

534   Sarah, C., and Patricia l, C.: Ground water vulnerability assessment: Predicting relative

535   contamination potential under conditions of uncertainty, National Academies Press, USA, 1993.

536   Secunda, S., Collin, M., and Melloul, A. J.: Groundwater vulnerability assessment using a

537   composite model combining DRASTIC with extensive agricultural land use in Israel's Sharon

538   region, J. Environ. Manage., 54, 39-57, https://doi.org/10.1006/jema.1998.0221, 1998.

539 Shirazi, S. M., Imran, H., and Akib, S.: GIS-based DRASTIC method for groundwater

540 vulnerability assessment: a review, J. Risk. Res., 15, 991-1011,

541 https://doi.org/10.1080/13669877.2012.686053, 2012.

542 Singh, A., Srivastav, S., Kumar, S., and Chakrapani, G. J.: A modified-DRASTIC model

543 (DRASTICA) for assessment of groundwater vulnerability to pollution in an urbanized

544 environment in Lucknow, India, Environ. Earth. Sci., 74, 5475-5490,

545 https://doi.org/10.1007/s12665-015-4558-5, 2015.

546 Souleymane, K., and Tang, Z.: A novel method of sensitivity analysis testing by applying the

547 DRASTIC and fuzzy optimization methods to assess groundwater vulnerability to pollution: the

548 case of the Senegal River basin in Mali, Nat. Hazards. Earth. Sys. Sci., 17, 1375-1392,

549 https://doi.org/10.5194/nhess-17-1375-2017, 2017.

550 Srivastava, P. K., and Bhattacharya, A. K.: Groundwater assessment through an integrated

551 approach using remote sensing, GIS and resistivity techniques: a case study from a hard rock

552 terrain, Int. J. Remote. Sens., 27, 4599-4620, https://doi.org/10.1080/01431160600554983,

553 2006.

554 Tilahun, K., and Merkel, B. J.: Assessment of groundwater vulnerability to pollution in Dire

555 Dawa, Ethiopia using DRASTIC, Environ. Earth. Sci., 59, 1485-1496,

556 https://doi.org/10.1007/s12665-009-0134-1, 2010.

557 Zghibi, A., Merzougui, A., Chenini, I., Ergaieg, K., Zouhri, L., and Tarhouni, J.: Groundwater

558 vulnerability analysis of Tunisian coastal aquifer: an application of DRASTIC index method in

559 GIS environment, Groundwater. Sustain. Develop., 2, 169-181,

560 https://doi.org/10.1016/j.gsd.2016.10.001, 2016.

561